

# Real Time Implementation of New Hybrid Non Integer Order Control Strategy in DC Motor Speed Control System

N.N.Praboo<sup>#1</sup>, P.K.Bhaba<sup>#2</sup>

<sup>#1</sup>Instrumentation Engineering Department, Annamalai University, Annamalai Nagar, INDIA

<sup>#2</sup>Chemical Engineering Department, Annamalai University, Annamalai Nagar, INDIA

**Abstract** — This paper deals with speed control of DC motor based on the design of new hybrid non integer order control strategy. This strategy is achieved by the peculiar hybridization of Fractional order  $PI^\lambda$  controller and CRONE third generation controller. Based on the mathematical model of DC motor armature voltage control, transfer function model is derived using real time specifications. Using the transfer function, Fractional order  $PI^\lambda$  controller and CRONE third generation controller are designed. The newly developed hybrid non integer order control strategy is compared with the above said controllers. Real time servo and regulatory runs are recorded and the results are tabulated. From the results the new hybrid non integer order controller has better results on par with other non integer controllers.

**Keywords** — Non-integer control, DC motor, CRONE, New Hybrid control, FO  $PI^\lambda$ , Stability Boundary Locus.

## I. INTRODUCTION

Modern day plants are more complex and more advanced in technology. So the old classical controllers are replaced by new robust controllers. Among the robust controllers non-integer order controllers have a special attention in the control society.

Fractional calculus is many centuries old, but only in recent years it gains its momentum due to the extensive work laid by many researchers in that field. The fractional order calculus finds its applications in many of the fields with wide vision.

Manabe [1] put forth a concept of non-integer order integral controller based on the idea of having a constant phase margin around a gain cross frequency.

This idea has been extended by Oustaloup and he studied fractional order control algorithms for the control of dynamic systems. Then he proposed a frequency domain based CRONE [2] controller (CRONE is a French acronym of “Comande Robuste d’Ordre Non Entier” which means non integer order robust controller).

Avoiding over estimation of plant disturbance leads CRONE to be a non-conservative robust

control system. The control of continuous and discrete time SISO and MIMO systems is also possible with CRONE strategy. The CRONE control strategy is classified into three generations are namely First, Second and Third CRONE controllers.

More recently Podlubny [3, 4] proposed a generalization of the PID controller, namely fractional  $PI^\lambda D^\mu$  controller. This controller gains popularity by imposing better flexibility, since it has two more tuning parameters which are the fractional integration action of order  $\lambda$  and the differentiation action order  $\mu$ .

The control of speed is considered to be an important issue and has been studied since the early decades in the last century. It has a wide application in industries such as electric vehicles, electric cranes, robotic manipulators and steel rolling mills due to its precise, simple and continuous characteristics.

In this work new hybrid non integer order controller is designed by hybridizing fractional order  $PI^\lambda$  and third generation CRONE controller in a fashion to achieve an improved performance in the control of DC motor speed [5].

The performance of this hybrid structure is compared with the individual performance of the fractional order  $PI^\lambda$  and third generation CRONE controller. The DC motor transfer function model is identified by substituting real time specifications in the derived mathematical model of armature voltage control of DC motor speed control system.

The organization of this article is as follows: The second section consists of armature voltage DC motor speed control mathematical model derivation and identification of transfer function model.

The third section explains about the design of Fractional Order (FO)  $PI^\lambda$  controller and third generation CRONE controller based on the previous section transfer function model.

The design of proposed new hybrid non integer order controller is discussed in the fourth section. Results are discussed in the section five. Section six consists of concluding remarks of this work.

II. DC MOTOR SPEED CONTROL SYSTEM

A. Real Time Interface

The real time set up of speed control DC motor is shown in Fig 1. The setup consists of DC motor, chopper driver unit, Opto-coupler sensor, V-MAT card and personal computer. The V-MAT card acts as a multifunction high speed data acquisition card to interface motor circuit with personal computing system.



Fig. 1. DC motor speed control real time setup

The real time system consists of a separately excited DC motor interfaced with PC through chopper circuit and V-MAT-01 motion control card. The V-MAT-01 card is helpful in interfacing the DC motor setup directly to Simulink tool of MATLAB® platform in the personal computer in order to run the real time control algorithms. The real time specifications are listed in Table 1.

TABLE 1. REAL TIME DC MOTOR SPECIFICATIONS

Parameters	Rating Values
Moment of Inertia of the rotor	J=0.03kgm <sup>2</sup>
Damping of the system	B=0.019 Nms
K <sub>b</sub> =K <sub>T</sub> =K	K=0.1331
Electric Resistance	R <sub>a</sub> =6Ω
Electric Inductance	L <sub>a</sub> =4.5 mH
Maximum Speed of motor	1500 rpm

B. Mathematical Model

The speed of DC motor is controlled by varying the armature voltage [6] of the motor coil. The control equivalent circuit of the DC motor by the armature voltage control method is shown in Fig. 2.

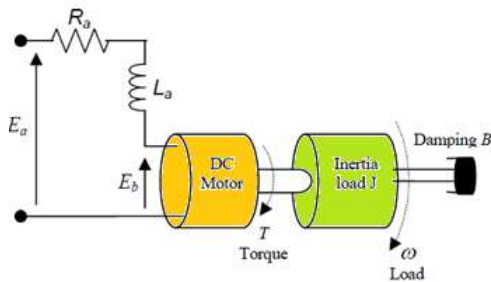


Fig. 2. Armature voltage DC motor speed control

The physical parameter of the DC motor dynamics is as follows: i<sub>a</sub>: armature current, (amp); i<sub>f</sub>: field current, (amp); ω: The speed of the shaft (angular velocity), (rad/s); e<sub>a</sub>: The input terminal voltage (source), (v); e<sub>b</sub>: The back EMF, (v); T<sub>m</sub>: The motor torque, (Nm); K<sub>T</sub>: The torque factor constant, (Nm/amp); K<sub>b</sub>: The motor constant, (v-s/rad).

Because the back EMF e<sub>b</sub> is proportional to speed ω directly, then

$$e_b(t) = K_b \frac{d\theta(t)}{dt} = K_b \omega(t) \tag{1}$$

$$e_a(t) = R_a i_a(t) + L_a \frac{di_a(t)}{dt} + e_b(t) \tag{2}$$

$$T_m(t) = J \frac{d^2\theta(t)}{dt^2} + B \frac{d\theta}{dt} = K_T i_a(t) \tag{3}$$

$$E_b(s) = K_b \omega(s) \tag{4}$$

$$E_a(s) = (R_a + L_a s) I_a(s) + E_b(s) \tag{5}$$

$$T_m(s) = J s \omega(s) + B \omega(s) = K_T i_a(s) \tag{6}$$

Fig. 3 describes the DC motor armature control system functional block diagram.

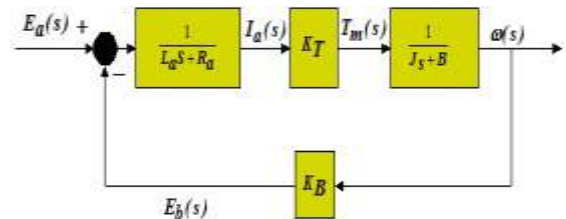


Fig. 3. Functional diagram of DC motor speed control

The transfer function of DC motor speed with respect to the input voltage can be written as follows,

$$G(s) = \frac{\omega(s)}{E_a(s)} = \frac{K_T}{(L_a s + R_a)(J s + B) + K_b K_T} \tag{7}$$

On substituting the real time values shown in Table 1, the transfer function model is obtained as follows.

$$G(s) = \frac{\omega(s)}{E_a(s)} = \frac{1.01}{0.001025s^2 + 1.367s + 1} \tag{8}$$

III. FO PI<sup>λ</sup> AND CRONE CONTROLLER DESIGN

A. FO PI<sup>λ</sup> Controller Design

The transfer function of such type of controller in Laplace domain has the form.

$$C_F(s) = K_p + \frac{K_i}{s^\lambda} + K_d s^\mu \tag{9}$$

The PI<sup>λ</sup>D<sup>μ</sup> algorithm is represented by a fractional integro-differential equation of type as follows

$$u(t) = K_p e(t) + K_i D^{-\lambda} e(t) + K_d D^\mu e(t) \tag{10}$$

D - Integro-Differential operator.

The transfer function of the FO PI<sup>λ</sup> controller is

$$C_F(s) = \frac{U(s)}{E(s)} = K_p + \frac{K_i}{s^\lambda} \quad (11)$$

This transfer function is obtained for K<sub>d</sub> = 0 in (9). The closed loop fractional order control system is shown in Fig. 4. The unity feedback control system consists of a plant G(s) and a controller C<sub>F</sub>(s). Consider the quasipolynomial fractional order transfer function of the plant [7].

$$G(s) = \frac{N(s)}{D(s)} = \frac{b_n s^{\beta_n} + b_{n-1} s^{\beta_{n-1}} + \dots + b_0 s^{\beta_0}}{a_n s^{\alpha_n} + a_{n-1} s^{\alpha_{n-1}} + \dots + a_0 s^{\alpha_0}}$$

$$= \frac{\sum_{i=0}^n b_i s^{\beta_i}}{\sum_{i=0}^n a_i s^{\alpha_i}} \quad (12)$$

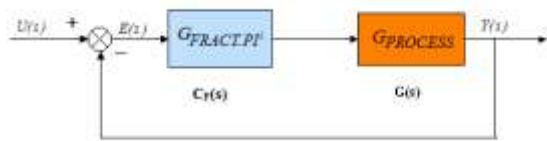


Fig. 4. Closed loop fractional order control system

The output of the unity feedback control system is given by

$$y = \frac{C_F(s)G(s)}{1 + C_F(s)G(s)} \bullet u \quad (13)$$

Where, u is the reference input and y is the output of the control system. The denominator of (12) represents the fractional order characteristic quasipolynomial (FOCQ) of the closed loop system. The set of all controller parameters are obtained by the formation of Global Stability (GS) region [8] based on stability boundary locus method. Therefore the designer has the set of all stabilizing controller parameters for the plant.

Substituting (11) and (12) in (13), The FOCQ is written as

$$P(s) = \sum_{i=0}^n [a_i(s)^{\alpha_i+\lambda} + K_p b_i(s)^{\beta_i+\lambda} + K_i b_i(s)^{\beta_i}] = 0 \quad (14)$$

Replacing s=jω and solving the above equation using mathematical identity by equating the real and imaginary parts to zero. The controller parameters obtained are

$$K_p = \frac{1}{\text{Sin}\left\{\left(\lambda\right)\left[\frac{\pi}{2}\right]\right\}} \frac{[A_1(\omega)B_2(\omega) - A_2(\omega)B_1(\omega)]}{[B_1^2(\omega) + B_2^2(\omega)]} \quad (15)$$

$$K_i = \frac{-\omega^\lambda}{\text{Sin}\left\{\left(\lambda\right)\left[\frac{\pi}{2}\right]\right\}} \frac{[A_3(\omega)B_2(\omega) - A_4(\omega)B_1(\omega)]}{[B_1^2(\omega) + B_2^2(\omega)]} \quad (16)$$

Using (15) and (16), a stability locus curve is drawn in the (K<sub>p</sub>-K<sub>i</sub>)-plane for any value of λ (ω changes from 0 to maximum (2)).

For the DC motor transfer function model (8), the test points inside and outside of the curve, the GS region is obtained λ for all values of (see Fig. 5). The goal is to obtain the GM of 4.5 dB and

PM of 20°. Since the DC motor system is stable and exhibits good dynamics in that region. The integral performance error indices are minimized in that region. These requirements are provided for the optimized values of the λ in the range of (1.15 to 1.25). Therefore, we choose λ=1.2 and determined the controller parameters as K<sub>p</sub>=1.5732, K<sub>i</sub>=1.45204 [9, 10]. So the Fractional order PI<sup>λ</sup> controller transfer function is found as

$$C_F(s) = 1.5732 + \frac{1.45204}{S^{1.2}} \quad (17)$$

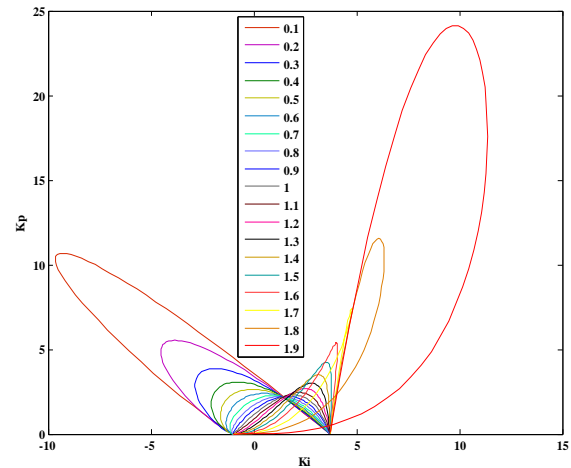


Fig. 5. Global stability region for different values of λ

### B. Third generation CRONE Controller Design

The CRONE controller design is a frequency domain approach. It is based on common unity feedback configuration. There are three generations of CRONE controller, out of which the third generation [11, 12 and 13] is the most advanced. The third generation CRONE can handle more general uncertainties. The third generation CRONE control strategy feedback structure is shown in Fig 6.

The third generation of CRONE control is based on the definition of a template which can be represented in the Nichols chart by any direction straight line segment around open loop gain crossover frequency ω<sub>cg</sub>. The complex fractional order integral transfer function with band-limited function is

$$\beta(s) = C^{\text{sign}(b)} \left(\frac{\omega_l}{s} + 1\right)^{n_l} \left(C_0 \frac{1+s/\omega_h}{1+s/\omega_l}\right)^a$$

$$\times \left( \text{Re}/i \left( C_0 \frac{1+s/\omega_h}{1+s/\omega_l} \right)^{ib} \right)^{-q \text{sign}(b)} \left( \frac{1}{\left(1 + \frac{s}{\omega_h}\right)^{n_h}} \right) \quad (18)$$

In the Nichols chart (see Fig. 7), the real order a determines the phase placement of the template, that is -Re/i(n) π/2 and the imaginary order b determines its angle to the vertical, at frequency ω<sub>cg</sub> imposed by the designer to obtain nominal performance.

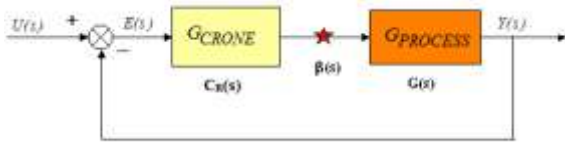


Fig. 6. Closed loop- CRONE control strategy

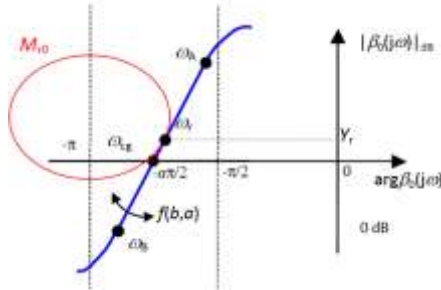


Fig. 7. Generalized template – Nichols locus

The third generation fractional order CRONE controller is

$$C_T(s) = \frac{\beta(s)}{G(s)} \quad (19)$$

There are eight high level parameters are there in open-loop complex fractional order integral transfer function  $\beta(s)$ , they are  $n_1, n_h, a, b, \omega_l, \omega_h, \omega_r$  and  $C$ . In which  $n_1$  and  $n_h$  are fixed by the control system designer (see Fig.8). In order to obtain the tangency condition,  $\omega_r$  and  $C$  are mentioned. A nonlinear optimization algorithm for the four independent parameters which minimizes the cost function  $J$  (20) based on the resonant peak variations and fulfils a set of shaping constraints [14, 15].

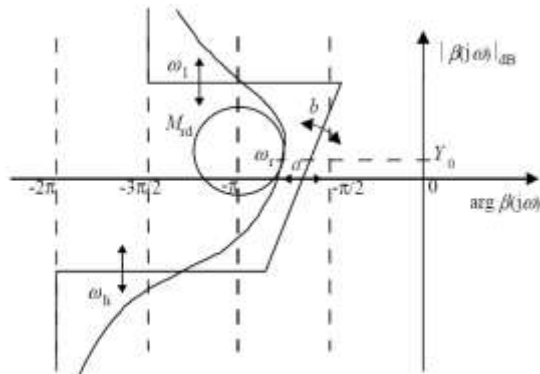


Fig. 8. Asymptotic Nichols locus

Synthesizing such a template through the optimization of three independent parameters (a tangency is imposed) from the four high-level parameters  $a, b, \omega_l$  and  $\omega_h$ , is the initial aim of the third generation CRONE control. The cost function minimized by the optimal template is

$$J = M_{rmax} - M_{r0} \quad (20)$$

The recursive distribution of real negative zeros and poles converts the fractional order band-limited transfer function into achievable rational order transfer function and it is represented as

$$C_R(s) = \frac{\beta_R(s)}{G(s)} \quad (21)$$

$$C_R(s) = \frac{C_0}{s^{N_{mr}}} \frac{\prod_{i=1}^{n_1} (1 + \frac{s}{\omega_{zi}})}{\prod_{i=1}^{d_1} (1 + \frac{s}{\omega_{pi}})} \frac{\prod_{i=1}^{n_2} (1 + \frac{2\zeta_{zi}s}{\omega_{nzi}} + \frac{s^2}{\omega_{nzi}^2})}{\prod_{i=1}^{d_2} (1 + \frac{2\zeta_{pi}s}{\omega_{npi}} + \frac{s^2}{\omega_{npi}^2})} \quad (22)$$

Based on DC motor transfer function and considering the initial assumptions in the design, the open loop complex band-limited fractional integral transfer function is obtained as

$$\beta(s) = 9.78 \text{sign}^{(0.28)} \left( \frac{0.6}{s} + 1 \right)^1 \left( 5 \frac{1+s/15}{1+s/0.6} \right)^{1.22} \times \left( \text{Re}/i \left( 5 \frac{1+s/15}{1+s/0.6} \right)^{i0.27} \right)^{-\text{sign}^{(0.278)} \left( \frac{1}{(1+\frac{s}{15})^3} \right)} \quad (23)$$

Further the rational optimized third generation CRONE controller transfer function is obtained as

$$C_R(s) = \frac{5.00187 (1 + \frac{s}{1710})}{s \left( 1 + \frac{s}{18.3} \right)} \times \frac{\left( 1 + \frac{2s}{1710} + \frac{s^2}{(1710)^2} \right) \left( 1 + \frac{2s}{0.555} + \frac{s^2}{(0.555)^2} \right)}{\left( 1 + \frac{2s}{18.3} + \frac{s^2}{(18.3)^2} \right) \left( 1 + \frac{2s}{18.3} + \frac{s^2}{(18.3)^2} \right)} \quad (24)$$

#### IV. NEW HYBRID NON-INTEGGER ORDER CONTROL

The proposed new hybrid non-integer order controller is obtained by hybridization of CRONE controller and Fractional Order  $PI^\lambda$  controller in a specified structure shown in fig 9.

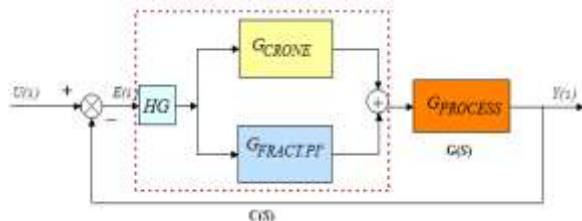


Fig. 9. New hybrid non-integer order control strategy

It is in series combination of both the controllers pre-multiplied by a hybrid gain. Process error  $E(s)$  is multiplied by hybrid gain before reaching the respective controllers. Each controllers output is added through a summing block and the additive control output is given to the final control element of the process.

An appropriate Hybrid gain is to be selected through a design process given in (25). Each controller is designed according to their design methods based on the model of the process.

It is a unification method of both non integer order control strategies. By doing so the control

performance is drastically improved in time domain, frequency domain and in error indices.

$$HG = \frac{K_p + C_0}{5} \quad (25)$$

$$HG = \frac{1.5732 + 5.0}{5} = 1.314 \quad (26)$$

Consider the design of fractional order  $PI^\lambda$  and CRONE controller design for the choice of Hybrid gain of the new modified hybrid non integer controller. In which the gain of the fractional order  $PI^\lambda$  is considered to be  $K_p$ , which is obtained from the design based on global stability region of the stability boundary locus for the value of optimized value of  $\lambda$ . Meanwhile the band-limited third generation CRONE controller gain  $C_0$  is obtained from the design of third generation CRONE controller. Substituting these values on the expression given above one can obtain the hybrid gain. That will provide a satisfactory performance for the new modified hybrid non integer controller.

### V. RESULTS AND DISCUSSIONS

Servo response (Set point tracking) of DC motor system is conducted at an operating point of 40% of speed in steps of +10%, +5%, -5% and -10% changes in speed in real time. The results are recorded shown in Fig. 10-13.

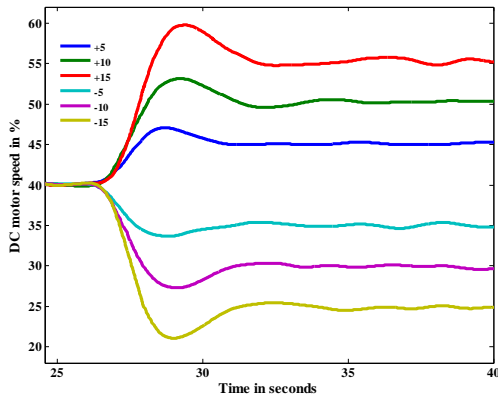


Fig. 10. Servo response of DC motor speed control system using Fractional Order  $PI^\lambda$  controller (Real Time)

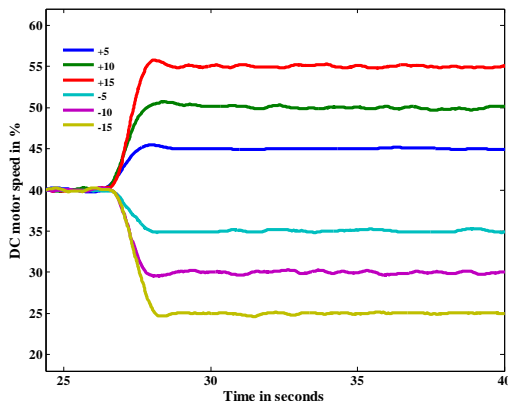


Fig. 11. Servo response of DC motor speed control system using Third generation CRONE controller (Real Time)

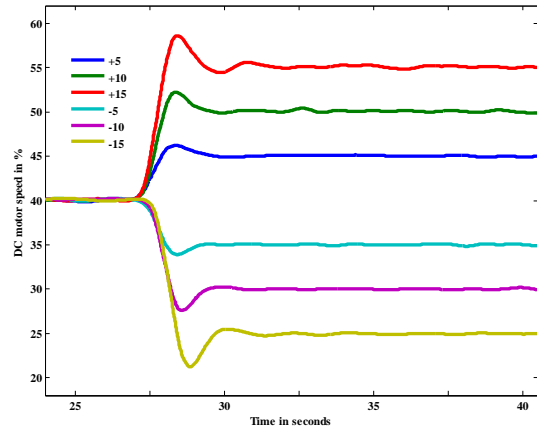


Fig. 12. Servo response of DC motor speed control system using New Hybrid non-integer order controller (Real Time)

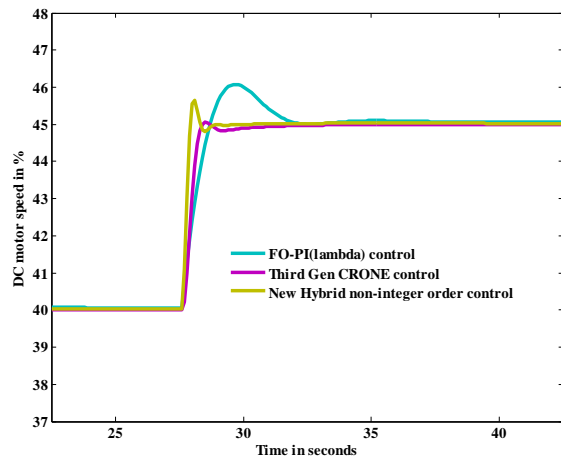


Fig. 13. Servo response of DC motor speed control system using all three control strategy at 40% set point speed to a step change of +5% speed

The results are recoded (Fig 10-12) and computed in terms of error indices performance. The error indices like Integral Squared Error (ISE) and Integral Absolute Error (IAE) are tabulated in Table 2.

TABLE 2. ERROR INDICES PERFORMANCE

Controllers	Indices	+10 %	+5 %	-5 %	-10 %
FO- $PI^\lambda$	ISE	2204	605	612	2339
	IAE	215	118	123	210
Third Gen. CRONE	ISE	2009	525	494	1979
	IAE	168	98	100	170
Hybrid	ISE	<b>1702</b>	<b>414</b>	<b>416</b>	<b>1817</b>
	IAE	<b>152</b>	<b>90</b>	<b>90</b>	<b>160</b>

The time domain performances for the response (Fig.13) are measured in the operating point of 40% speed with 5% step change and the results are tabulated in Table 3.

TABLE 3. TIME DOMAIN PERFORMANCE

Controllers	Settling Time $t_s$ (Secs)	Rise Time $t_r$ (Secs)	Peak Overshoot % Mp
FO- PI <sup>λ</sup>	39	30	2.888
Third. Gen CRONE	34	28	0.555
Hybrid	<b>28</b>	<b>27</b>	1.555

In the time domain performance measures the new hybrid non-integer order controller peak overshoot is slightly greater than CRONE, but it is well below the admissible range. Moreover the other performances are drastically improved compared to other control strategy.

### VI. CONCLUSION

In this paper a proposed new hybrid non-integer order controller is designed using hybridization technique of both Fractional PI<sup>λ</sup> and third generation CRONE controller in a specified structure. It is a unification technique of two different robust control strategies into a single structure of controller. From the time domain and error indices performance measures, it is inferred that the proposed new hybrid non-integer order controller outperforms the other non integer controllers.

### REFERENCES

[1] S. Manabe. , The non-integer integral and its application to control systems, *Japanese institute of electrical engineers journal*, 80(860): 589-597, 1960.

[2] A. Oustaloup, *La commande CRONE*, Editions HERMES, Paris, 1991.

[3] I. Podlubny, Fractional-order systems and PI<sup>λ</sup>D<sup>μ</sup>-controllers, *IEEE Trans. Autom. Control*, vol. 44, no. 1, pp. 208–214, 1999.

[4] I. Podlubny, *Fractional Differentiation Equations*, Academic Press, San Diego, 1999.

[5] Guoshing Huang and Shuocheng Lee, PC-based PID Speed Control in DC Motor, *IEEE, ICALIP*, 2008.

[6] Baek S. M. and T. Y. Kuc, An adaptive PID learning control of DC motor., *IEEE International*. 3: 2877-2882, 1997.

[7] N. N. Praboo, P K. Bhaba and S.E. Hamamci, Fractional Order PI<sup>λ</sup> control strategy for a Liquid level system, *IEEE proceedings of world congress on Nature and Biologically Inspired Computing*, Kitakyushu, Japan, pp. 121-126, 2010.

[8] S. E. Hamamci, Stabilization using fractional-order PI and PID controllers, *Nonlinear Dynamics*, vol. 51, pp. 329-343, 2008.

[9] A. Monje, Yang Quan Chen, Blas M. Vinagre, Dingyu xue and Vicente Feliu, Fractional Order systems and controls: Fundamentals and applications, *Advances in industrial control*, Springer, 2010.

[10] N.N. Praboo, P.K. Bhaba, Simulation work on Fractional order PI<sup>λ</sup> control strategy for speed control of DC motor based on stability boundary locus method, *International Journal of Engineering Trends and Technology*, Vol 4(8), pp. 3403-3409, 2013.

[11] A. Oustaloup, B. Mathieu and P. lanusee, Third generation CRONE control, *IEEE international conference on systems, man and cybernetics*, Le Touquet. 17-20 October, France. pp. 149-155, 1993.

[12] A. Oustaloup, B. Mathieu and P. lanusee, The Great principles of the CRONE control, *IEEE international*

*conference on systems, man and cybernetics*, Le Touquet. 17-20 October, France. pp. 118-129, 1993.

[13] A. Oustaloup, X. Moreau and M. Nouillant, The CRONE suspension, *Control engineering Practice*, 4(8): 1101-1108, 1996.

[14] A. Oustaloup, P. Melchior, P. Lanusse, O. Cois and F. Dancla, The CRONE tool box for MATLAB, *IEEE international symposium on Computer aided control system Design*, Anchorage, Alaska, USA, September 25-27, 2000.

[15] CRONE tool box, *CRONE research group*, Universite de Bordeaux, France.